Photoelectron spectroscopy of GaX_2^-, Ga_2X^-, $Ga_2X_2^-$, and $Ga_2X_3^-$ (X=P,As)

Travis R. Taylor,[a] Harry Gómez, Knut R. Asmis,[b] and Daniel M. Neumark
Department of Chemistry, University of California, Berkeley, California 94720 and Chemical Sciences Division, Lawrence Berkeley National Laboratory, Berkeley, California 94720

(Received 16 May 2001; accepted 19 June 2001)

Anion photoelectron spectra taken at various photodetachment wavelengths have been obtained for GaX_2^-, Ga_2X^-, $Ga_2X_2^-$, and $Ga_2X_3^-$ (X=P,As). The incorporation of a liquid nitrogen cooled channel in the ion source resulted in substantial vibrational cooling of the cluster anions, resulting in resolved vibrational progressions in the photoelectron spectra of all species except $Ga_2X_2^-$. Electron affinities, electronic term values, and vibrational frequencies are reported and compared to electronic structure calculations. In addition, similarities and differences between the phosphorus and arsenic-containing isovalent species are discussed.
[DOI: 10.1063/1.1391267]

I. INTRODUCTION

Since the invention of the transistor in 1947, semiconductor materials have become an essential part of the electronics industry. Group III–V materials have shown particular promise as semiconductors and have demonstrated a variety of novel characteristics.[1] While bulk semiconductor materials have been thoroughly studied and are well understood, small molecules made of group III–V elements have received relatively little attention despite their importance in processes such as epitaxial growth and chemical vapor deposition. It has been a goal of our research group to characterize the electronic and vibrational structure of clusters formed from bulk semiconducting materials. This study represents continued progress towards this goal by investigating the electronic and vibrational structure of GaX_2^-, Ga_2X^-, $Ga_2X_2^-$, and $Ga_2X_3^-$ (X=P,As) clusters via anion photoelectron spectroscopy.

Several gas phase and matrix experiments have been carried out in order to characterize the electronic and vibrational spectroscopy of polyatomic Ga_xX_y species. The first systematic experimental studies were carried out by Smalley and co-workers,[2–4] in which Ga_xAs_y neutral and anionic clusters with up to 50 atoms were generated by laser ablation and characterized in photodissociation, photodetachment, and photoelectron (PE) spectroscopy experiments. PE spectra of mass-selected $Ga_xAs_y^-$ anion clusters showed an even–odd alternation in electron affinities and provided information on the excited state energetics of the neutral clusters.[4] However, the mass resolution was not sufficient to separate clusters with the same number of atoms but differing stoichiometry, and the electron energy resolution (>100 meV) was sufficient to resolve electronic structure only. Li *et al.*[5] have carried out infrared matrix infrared absorption experiments revealing and measured vibrational frequencies of GaX, GaX_2, and Ga_2X(X=P,As). These authors also measured the electron spin resonance spectrum of Ga_2As_3 in a matrix and concluded that it has a trigonal bipyramidal structure with the unpaired electron shared between the two gallium atoms.[6] Electric dipole polarizabilities of gallium arsenide clusters have been measured by Schlect *et al.*[7]

Taylor *et al.* have carried out two studies on $Ga_xP_y^-$ clusters via anion PE spectroscopy. They obtained vertical detachment energies from the PE spectra of size-selected clusters $Ga_xP_y^-$ ($x+y \leq 18$) at a photon wavelength of 266 nm and an energy resolution of 30 meV.[8] This study showed an odd–even alternation in electron affinities consistent with the open-shell/closed-shell structure of the clusters, similar to the trend seen by Jin *et al.*[4] for Ga_xAs_y clusters. The size-dependence of electron affinities for the Ga_xP_y clusters could be readily extrapolated to the bulk value, a trend also observed in In_xP_y clusters.[9] In a more recent, higher resolution (10 meV) study, Taylor *et al.*[10] published preliminary vibrationally-resolved PE spectra of GaP_2^-, Ga_2P^-, and $Ga_2P_3^-$ anions and concluded that the anion ground state and the neutral states of GaP_2 and Ga_2P are bent C_{2v} structures. The ground and two excited states of GaP_2 were assigned based on comparison to *ab initio* calculations by Feng and Balasubramanian,[11] but assignment of the Ga_2P^- photoelectron spectrum was more problematic. No vibrational structure was seen in the $Ga_2P_2^-$ PE spectrum at 10 meV resolution, an interesting result given the observation of vibrational structure in the PE spectra of Si_4^- (Refs. 12, 13) and $Ga_2P_3^-$ taken at comparable resolution.

Several theoretical descriptions of polyatomic GaX (X=P,As) clusters have been carried out. Balasubramanian and co-workers have performed a series of complete active space self-consistent field (CASSCF) and multireference singles and doubles configuration interaction (MRSDCI) calculations, finding geometries and term values for neutral and charged (mainly cationic) gallium arsenide[14–20] and gallium phosphide[11,21–23] clusters with up to five atoms. Graves

[a]Current address: Lam Research, 47131 Bayside Parkway, Fremont, California 94538.
[b]Also at Arnimallee 14, Institut fur Experimentalphysik, Fachbereich Physik, Freie Universitat Berlin, D-14195, Berlin, Germany.

et al.[24] and Al-Laham *et al.*[25] have carried out *ab initio* calculations to determine the ground state of the 1:1 stoichiometric $(GaAs)_n$ clusters with up to 8 atoms. Lou *et al.*[26,27] calculated structures of stoichiometric and nonstoichiometric Ga_xAs_y clusters using the local spin density method. Andreoni carried out Car–Parrinello molecular dynamics calculations to study the structures, stability and melting of small stoichiometric GaP, GaAs, and AlAs clusters;[28] a more recent study by Tozzini *et al.*[29] on larger GaP clusters showed evidence for fullerenelike structures for clusters with as few at 20 atoms. Meier *et al.*[30] investigated neutral, cationic, and anionic $GaAs_2$ and Ga_2As_2 clusters in a multireference configuration interaction (MRD-CI) calculation. Archibong and St. Amant[31] have used coupled cluster singles and doubles (CCSD(T)) and Becke-3-parameter-Lee-Yang-Parr (B3LYP) theoretical methods to study GaP and GaP_2, calculating term energies and vibrational frequencies of the neutral and anion states. These authors have also found that the ground state of $Ga_2P_2^-$ has a nonplanar geometry with C_{2v} symmetry,[32] in contrast to the planar rhombic (D_{2h}) ground state of neutral Ga_2P_2, and propose this change in geometry to be origin for the absence of vibrational structure in the $Ga_2P_2^-$ PE spectrum. In support of the electron spin resonance experiment by Van Zee,[6] Arratia-Perez *et al.*[33,34] have calculated the paramagnetic resonance parameters for Ga_2As_3, Ga_2As, and $GaAs_2$. The electronic absorption spectrum of these and other GaAs clusters was recently calculated by Vasiliev *et al.*[35]

Here we present vibrationally-resolved anion PE spectra of GaX_2^-, Ga_2X^-, $Ga_2X_3^-$(X=P,As) clusters and we also discuss the electronic structure of Ga_2X_2. The addition of a liquid nitrogen cooled clustering channel to our laser ablation disc source results in vibrationally cooler anion cluster precursors than in previous work. This significantly improves the quality of our photoelectron spectra and allows us to more accurately report electron affinities, vibrational frequencies, and term values. The assignment of these spectra is also aided by comparison to our recently reported PE spectra of $Al_xP_y^-$ clusters.[36]

II. EXPERIMENT

The anion photoelectron spectrometer used in this study has been described in detail previously.[37,38] Cluster anions are generated in a laser ablation/pulsed molecular beam source equipped with an additional liquid nitrogen cooled clustering channel as shown in Fig. 1. The piezoelectric molecular beam valve (a) releases a helium gas pulse which intercepts the resulting clusters generated by ablating a rotating and translating single crystal disk (b) of GaP or GaAs (Crystallode Inc.) with the second harmonic (532 nm) of a pulsed Nd:YAG laser (c). The laser pulse energies are typically 5.0–7.5 mJ/pulse and are focused onto the target with a 50 cm lens. The gas pulse continues to travel through a 1.75 in. long copper clustering channel (e). The copper channel is cooled by gravimetrically flowing liquid nitrogen through 1/8 in. diam copper tubing in thermal contact with the channel. To prevent the valve from cooling, a 1/4 in. thick insulator (d) made of Delrin is located between the copper channel and the laser ablation assembly. In addition, the laser ablation assembly is heated enough to maintain it at room temperature. Thermocouples are used to ensure that the clustering channel and molecular beam valve are maintained at the appropriate temperatures. The gas pulse exits the clustering channel and passes through a skimmer into a differentially pumped region. Negative ions in the beam are extracted perpendicular to their flow direction by a pulsed electric field and injected into a linear reflectron time-of-flight (TOF) mass spectrometer[39,40] with a mass resolution $m/\Delta m$ of 2000. Due to the natural isotope abundance of gallium (Ga^{69}:Ga^{71}, 100.0:66.4) each cluster stoichiometry has a mass distribution that is fully resolved in our instrument. In each case the most intense mass peak was photodetached.

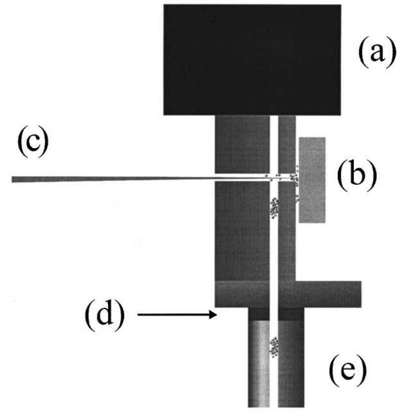

FIG. 1. Diagram of the liquid nitrogen cooled clustering channel coupled with the laser ablation disk source. The diagram is labeled as follows: (a) pulsed piezoelectric valve, (b) disk ablation target, (c) incident laser beam, (d) Delrin insulating disk, and (e) copper clustering channel.

The ion of interest is selectively photodetached at a photon wavelength of 355 nm (3.493 eV), 416 nm (2.977 eV), or 498 nm (2.490 eV). The 355 nm wavelength is obtained by tripling the fundamental of a pulsed Nd:YAG laser, while light at 416 and 498 nm corresponds to the first and second Stokes lines generated by passing the laser pulse at 355 nm through a high pressure Raman cell filled with hydrogen at 325 psig. The electron kinetic energy (eKE) distribution is determined by TOF analysis in a 1 m field-free flight tube. The energy resolution is 8–10 meV at 0.65 eV eKE and degrades as $(eKE)^{3/2}$ at higher eKE. The data in electron kinetic energy is converted to electron binding energy (eBE) by subtracting it from the photon energy. All data are plotted in eBE as described by Eq. (1), where EA is the adiabatic electron affinity, E^o is the internal energy of the neutral, and E^- is the internal energy of the anion,

$$\mathrm{eBE}=h\nu-\mathrm{eKE}=\mathrm{EA}+E^o-E^-. \quad (1)$$

The angular dependence of the photodetachment intensity for polarized light and randomly oriented molecules is given by Eq. (2) below,[41]

$$\frac{d\sigma}{d\Omega}=\frac{\sigma_{\mathrm{total}}}{4\pi}\left[1+\frac{\beta(\mathrm{eKE})}{2}(3\cos^2\theta-1)\right], \quad (2)$$

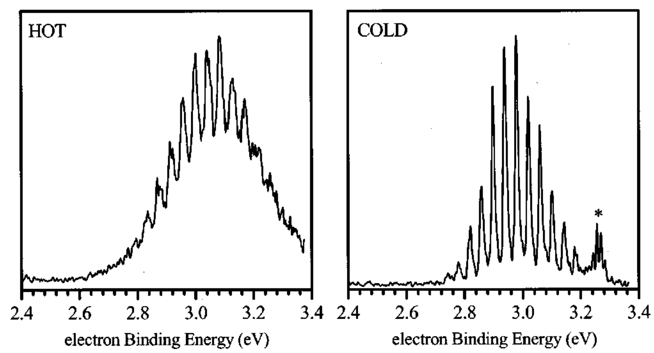

FIG. 2. Comparison of ''hot'' and ''cold'' anion photoelectron spectra of GaP_2^- taken at a wavelength of 355 nm and polarization angle of $\theta=0°$. The spectrum shows only the $\tilde{A}\ ^2A_1$ state of GaP_2.

where θ is the angle between the electric vector of the photon and the direction of electron ejection, σ_{total} is the total photodetachment cross section and β(eKE) is the asymmetry parameter $(-1\leqslant\beta\leqslant2)$. Each electronic state typically has a characteristic asymmetry parameter and this can be used to distinguish contributions from overlapping electronic transitions. The anisotropy parameter of a peak is calculated[42] using Eq. (3),

$$\beta=\frac{I_{0°}-I_{90°}}{\frac{1}{2}I_{0°}+I_{90°}}, \tag{3}$$

where $I_{0°}$ and $I_{90°}$ are the intensities of the peak taken at the polarization angles $\theta=0°$ and 90°. The laser polarization can be rotated with respect to the direction of electron detection by using a half-wave plate.

III. RESULTS

Figure 2 shows a portion of the 355 nm GaP_2^- photoelectron spectrum taken at room temperature (HOT) and with liquid nitrogen cooling of the clustering channel (COLD). The HOT spectrum was reported in our earlier work[10] and was assigned to the transition to the $\tilde{A}(^2A_1)$ excited state of GaP_2. These two spectra demonstrate our ability to vibrationally cool the anions prior to photodetachment, yielding a much better-resolved PE spectrum. All spectra reported below were taken under cold conditions.

Figures 3–6 show the anion photoelectron spectra of GaX_2^-, Ga_2X^-, $Ga_2X_2^-$, and $Ga_2X_3^-$(X=P,As), respectively. For all spectra the ordinate is intensity with arbitrary units and the abscissa is in electron binding energy (eBE) with units of eV. Spectra of $Ga_xP_y^-$ and $Ga_xAs_y^-$ clusters with the same stoichiometry are in general quite similar, the main exception being the excited state (high eBE) bands in Figs. 4 and 5 for Ga_2P and Ga_2As. This similarity also extends to the photoelectron angular distributions, as can be seen by visual comparison of spectra taken at the same photodetachment wavelength but different laser polarization angles. Where possible β has been determined and for GaX_2 these values are located in Tables I and II. The values of β for Ga_2X are shown graphically in Fig. 4 and Ga_2X_3 angular distributions are discussed Sec. IV D. The features marked with the asterisk (*) appear only in the Ga_2X and GaX_2 spectra. They are observed in the ''cold'' spectra of Ga_2X^- and GaX_2^- but are obscured in the ''hot'' spectra. They are most significant in the gallium arsenide species and are not significant in spectra taken at 266 nm. Comparison to the PE spectra of GaP^- and $GaAs^-$ suggests these features are most likely due to photodissociation to GaX^- followed by photodetachment of the diatomic anion.[43]

Figure 3 shows six panels corresponding to the GaX_2^- spectra taken at different wavelengths and polarization angles. The top panels for each species display the spectra taken at 498 cm^{-1} and $\theta=90°$. The lower two panels show spectra taken at 355 nm and $\theta=90°$ and 0°. The spectra are comprised of two well-separated bands corresponding to

TABLE I. Comparison of geometries and energy separations of GaP_2/GaP_2^-.

Reference	Species	State	Level	θ (°)	Ga–P (Å)	P–P (Å)	ΔE (eV)	$\nu_1(a_1)$	$\nu_2(a_1)$	$\nu_3(b_2)$	β_{355}
Feng *et al.*[a]	GaP_2	$^2B_2$	MRSDCI	43.9	2.658	1.987	0.0				
	GaP_2	$^2A_1$	MRSDCI	56.0	2.308	2.167	1.07				
	GaP_2	$^2B_1$	MRSDCI	55.8	2.400	2.246	2.33				
Archibong *et al.*[b]	GaP_2^-	$^1A_1$	B3LYP	48.9	2.481	2.056	−1.73(−1.75)	590	260	240	
	GaP_2	$^2B_2$	B3LYP	43.6	2.657	1.972	0.0(0.0)	690	210	139	
	GaP_2	$^2A_1$	B3LYP	54.9	2.311	2.129	0.98(0.78)	532	328	355	
	GaP_2	$^2B_1$	MP2-F19[c]	49.8	2.574	2.168	2.81(2.55)	513	247	249	
Theory	GaP_2^-	$^1A_1$	B3LYP	48.9	2.490	2.061	−1.722	584	258	237	
	GaP_2	$^2B_2$	B3LYP	43.5	2.667	1.980	0	685	208	137	
	GaP_2^-	$^2A_1$	B3LYP	54.9	2.317	2.135	0.997	526	326	349	
Experiment[d]	GaP_2^-	$^1A_1$	PES				−1.666±0.041	589			
	GaP_2	$^2B_2$	PES				0.0		222		−0.81
	GaP_2	$^2B_2$	MATRIX[e]	52			0.0	322[f]	220.9		
	GaP_2	$^2A_1$	PES				1.044±0.101		328		+0.18
	GaP_2	$^2B_1$	PES				2.603±0.051	500	234		

[a]Reference 11.
[b]Reference 31. CCSD(T)-FC//B3LYP value in parentheses. Frequencies calculated with B3LYP.
[c]CCSD(T)//MP2-F19 values in parentheses. Frequencies calculated with MP2-F19.
[d]This work, except as noted.
[e]Reference 5.
[f]See discussion in text.

TABLE II. Comparison of geometries and energy separations of $GaAs_2/GaAs_2^-$.

Reference	Species	State	Level	θ (°)	Ga–As (Å)	As–As (Å)	ΔE (eV)	$\nu_1(a_1)$	$\nu_2(a_1)$	$\nu_3(b_2)$	β_{355}
Balasubramanian[a]	$GaAs_2^-$	$^1A_1$	MRSDCI	52.7	2.586	2.296	−1.50(−1.61)	329.6	198.1	152.1	
	$GaAs_2$	$^2B_2$	MRSDCI	45.9	2.80	2.184	0.0	382.5	162.5	80.3	
	$GaAs_2$	$^2A_1$	MRSDCI	60.7	2.4	2.425	0.71(0.65)	311.6	238.7	161.9	
	$GaAs_2$	$^2B_1$	MRSDCI								
Meier[b]	$GaAs_2^-$	$^1A_1$	FCIe	49.6	2.73	2.29	−1.42				
	$GaAs_2$	$^2B_2$	FCIe	46.6	2.27	2.87	0.0				
	$GaAs_2$	$^2A_1$	FCIe	58.4	2.44	2.50	0.65				
Theory	$GaAs_2^-$	$^1A_1$	B3LYP	52.2	2.601	2.290	−1.856	331	200	150	
	$GaAs_2$	$^2B_2$	B3LYP	46.4	2.783	2.195	0.000	381	166	87	
Experiment[c]	$GaAs_2^-$	$^1A_1$	PES				−1.894±0.033				
	$GaAs_2$	$^2B_2$	PES				0.0		176		−0.65
	$GaAs_2$	$^2B_2$	MATRIX[d]	38			0.0		174.1		
	$GaAs_2$	$^2A_1$	PES				0.694±0.077		235		+0.70
	$GaAs_2$	$^2B_1$	PES								

[a]Reference 11. Values in parenthesis are MRSDCI+Q.
[b]Reference 30.
[c]This work, except as noted.
[d]Reference 5.

transitions to the ground and first excited states of GaX_2. Based on comparison with *ab initio* calculations by Feng,[11] we concluded previously that the anion ground state and neutral states of GaP_2 have C_{2v} geometries and assigned the ground and first excited states to the $\tilde{X}\,^2B_2$ and $\tilde{A}\,^2A_1$ states, respectively.[8,10] This assignment is consistent with more recent calculations by Archibong.[31] Given the similarities between the spectra of GaP_2 and $GaAs_2$ the same assignments should apply to $GaAs_2$. Further support for this assignment is provided in Sec. IV A. Both states of GaX_2 exhibit similar extended vibrational progressions, implying a significant geometry change between the anion and neutral states. The $\tilde{X}\,^2B_2$ and $\tilde{A}\,^2A_1$ bands in the GaP_2^- spectra show vibrational progressions with frequencies of 222 and 328 cm^{-1}, respectively. In the $GaAs_2^-$ spectra, the frequencies associated with the $\tilde{X}\,^2B_2$ and $\tilde{A}\,^2A_1$ bands are 176 cm^{-1} and 235 cm^{-1}, respectively, with a somewhat irregular intensity distribution in the $\tilde{A}\,^2A_1$ band. Comparison of the 355 nm spectra at $\theta=0°$ and 90° indicates a strongly negative anisotropy parameter for detachment to the ground state for both species (see Tables I and II).

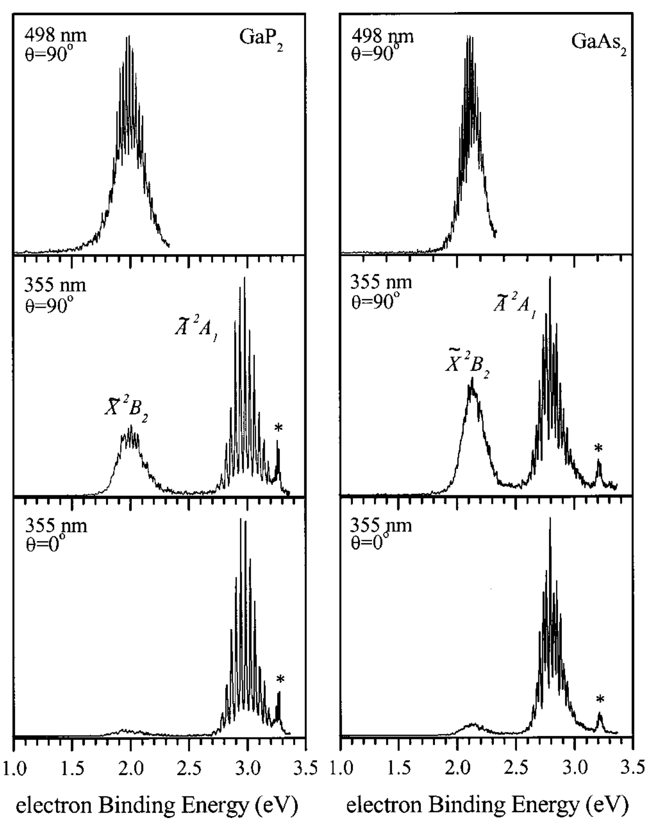

FIG. 3. Anion photoelectron spectra of GaX_2^- (X=P,As) taken at the wavelengths and polarization angles indicated. The features marked with an asterisk (*) are discussed in the text.

The PE spectra of Ga_2P^- and Ga_2As^- in Fig. 4 taken at 355 nm each show two distinct bands: a narrow band (X) with no resolved vibrational structure and a higher energy band with some resolved structure. Spectra of band X taken at 416 nm also showed no vibrational structure. Comparison of the intensities at $\theta=0°$ and 90° as well as an examination of the anisotropy parameters β, shown graphically for each peak in the top panels of Fig. 4, indicate that the higher energy feature is composed of two overlapping transitions labeled A and B in Fig. 4, with A having a more positive anisotropy parameter. Band A is vibrationally resolved for both species. Band B in the Ga_2P^- spectra is a broad, unresolved feature while it is structured in the Ga_2As^- spectra. The Ga_2P^- spectra are quite similar to the Al_2P^- spectra obtained at 355 nm.[36] In Fig. 4, feature A of Ga_2P has the best-resolved vibrational structure yielding a neutral frequency of 328 cm^{-1}. A hot band transition, labeled as a, gives us an anion frequency of 385 cm^{-1}. It is more difficult to extract vibrational frequencies from the overlapped bands A and B in the Ga_2As^- spectra, but band A is more prominent at $\theta=0°$ and the first four peaks of this peak are spaced by 279 cm^{-1}. A more quantitative analysis of this band is presented in the next section.

The use of a cooling channel did not result in the vibrationally-resolved PE spectra for the four-atom clusters

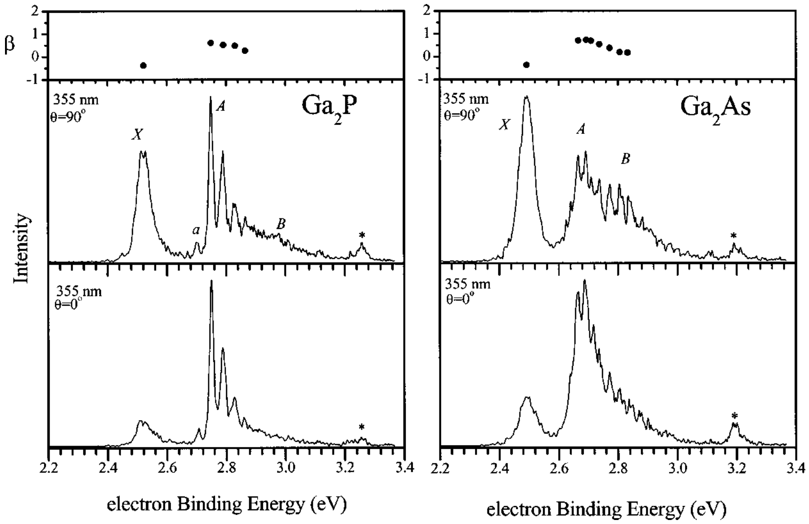

FIG. 4. Anion photoelectron spectra of Ga_2X^- (X=P,As) taken at a wavelength of 355 nm and polarization angles of θ=0° and 90°. The plot of the β parameters is located in the top panel. The features marked with an asterisk (*) are discussed in the text.

$Ga_2X_2^-$. Figure 5 shows the anion photoelectron spectra of $Ga_2X_2^-$ taken at 355 nm and θ=0°. Spectra were taken at other polarization angles, but the θ=0° spectra are optimal for showing the important spectral features. The spectra show a weak band at low eBE (labeled X) and a stronger band (*A*) at higher eBE. These spectra resemble those for $Al_2P_2^-$, the main difference being that the band at higher eBE is vibrationally resolved for $Al_2P_2^-$.[36]

We are able to resolve vibrational structure in the photoelectron spectra of $Ga_2X_3^-$. Figure 6 shows the photoelectron spectra taken at a wavelength of 355 nm and polarization angles of θ=0° and 90°. The spectra taken at θ=90° (top panel) shows one electronic state (band *X*) with an extended progression having a frequency of 213 and 193 cm^{-1} in Ga_2P_3 and Ga_2As_3, respectively. There is additional non-negligible intensity extending toward lower binding energy, more pronounced for Ga_2P_3 than for Ga_2As_3. The low eBE signal is more intense in θ=0° spectra for both species and appears to consist of two contributions labeled *a* and *b*. The 266 nm spectrum (dotted line) of $Ga_2P_3^-$ taken at θ=0° is shown superimposed on the 355 nm spectra in the lower panel. Peaks *a* and *b* do not appear in the 266 nm spectrum of $Ga_2P_3^-$.

IV. ANALYSIS AND DISCUSSION

In this section, the electronic bands and vibrational progressions seen in the $Ga_xP_y^-$ and $Ga_xAs_y^-$ PE spectra will be assigned. This process is facilitated by comparison with electronic structure calculations. As discussed in the Introduction, calculations have been performed previously on some of the clusters studied in this paper; the electronic state energies, geometries, and (when available) vibrational frequencies from this earlier work are summarized in Tables I–V. While these calculated parameters could be directly compared to the experimental PE spectra, it is also very useful to be able to simulate the PE spectra based on electronic structure calculations, and for this the normal coordinate displacements between the anion and various neutral electronic states are needed. Since the force constants required to calculate these displacements are typically not reported, we have carried out our own electronic structure calculations for the anionic and neutral ($x=1$, $y=2$), (2,1), and (2,3) gallium phosphide and arsenide clusters.

These calculations were performed using the GAUSSIAN 98 (Ref. 44) program package. Calculations with GAUSSIAN were performed on the Cray J90 SE cluster at the

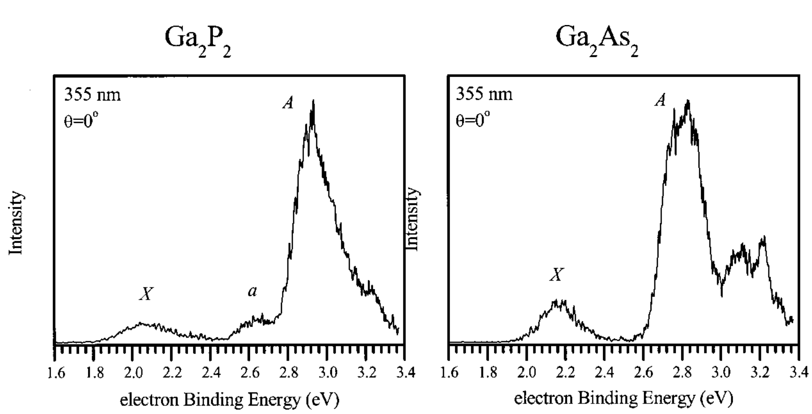

FIG. 5. Anion photoelectron spectra of $Ga_2X_2^-$ (X=P,As) taken at a wavelength of 355 nm and polarization angle of θ=0°.

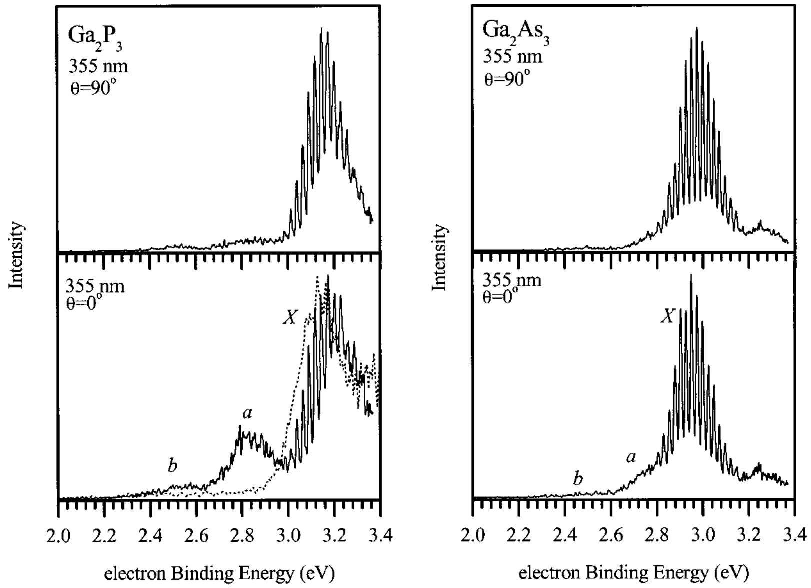

FIG. 6. Anion photoelectron spectra of $Ga_2X_3^-$ (X=P,As) taken at a wavelength of 355 nm and polarization angles of $\theta=0°$ and 90°. The dotted line in the lower left panel was taken at 266 nm.

National Energy Research Scientific Computing Center at the Lawrence Berkeley National Laboratory. The correlation consistent polarized valence basis sets of Dunning and co-workers,[45] denoted by cc-pVxZ where $x=$D (double zeta) and T (triple zeta) were used. Additional diffuse functions are especially important for the description of molecular ions and we therefore mostly used augmented correlation consistent sets of Kendall *et al.*,[46] denoted by aug-cc-pVxZ ($x=$D,T). The geometries and vibrational frequencies were determined using density functional theory (DFT) with the B3LYP (Becke-3-parameter-Lee-Yang-Parr) exchange correlation functional.[47,48] Except for the (1,2) clusters, only ground states of the neutral clustes were calculated. In light of the previous calculations on these species, only structures with C_{2v} symmetry were considered for the triatomic neutral and anionic species. A search for structural isomers of the Ga_2X_3 anionic and neutral clusters with C_s or C_{2v} symmetry was carried out using lower level HF/6-311G and B3LYP/6-311G calculations, but trigonal bipyramidal geometries with D_{3h} symmetry were always found to correspond to the minimum energy structure. Hence calculations at the higher level of theory described above were restricted to D_{3h} symmetry.

Our results are listed in Tables I–V. The tables include normal coordinate displacements ΔQ_i, which were calculated using the parallel mode approximation with the anion force constants. This approach allows us to calculate the ΔQ_i's for detachment to neutral excited states for which geometries are available from earlier calculations; these values are also listed in Tables I–V. Comparison with earlier work shows that our calculations are generally in good agreement with those of Archibong *et al.*,[31] as expected since the level of theory used in both sets calculations was similar. Agreement with the MRSDCI calculations of Balasubramanian[11,20] is reasonable for GaX_2 and Ga_2X_3 but less so for Ga_2X species (see Tables III and IV).

Franck–Condon (FC) simulations of the photoelectron spectra were carried out within the parallel-mode approximation assuming harmonic oscillator potentials. Starting from the parameters obtained from the calculations in Tables I–V, electronic state energies, vibrational frequencies, and normal coordinate changes used as input to the simulations were optimized to best reproduce the experimental PE spectra. The simulations are particularly important for extended progressions where the origin of the state is not definitively

TABLE III. Comparison of geometries and energy separations of Ga_2P/Ga_2P^-.

Reference	Species	State	Level	θ (°)	Ga–P (Å)	Ga–Ga (Å)	ΔE (eV)	$\nu_1(a_1)$	$\nu_2(a_1)$	$\nu_3(b_2)$
Feng *et al.*[a]	Ga_2P	$^2B_1$	MRSDCI	111.0	2.419		0.0			
	Ga_2P	$^2B_2$	MRSDCI	90.0	2.300		0.09			
	Ga_2P	$^2\Pi_u$	MRSDCI	180.0	2.391		0.16			
Theory	Ga_2P^-	$^1A_1$	B3LYP	108.2	2.283	3.700	−2.449	323	56	396
	Ga_2P	$^2B_2$	B3LYP	99.9	2.282	3.496	0.000	312	57	173*i*
Experiment[b]	Ga_2P^-	$^1A_1$	PES				-2.481 ± 0.015	$375\pm$ 25		
	Ga_2P	*X*	PES				0.0			
	Ga_2P	*X*	MATRIX	85.7			0.0			280.5
	Ga_2P	*A*	PES				0.268 ± 0.025	311		
	Ga_2P	*B*	PES				~0.4[e]			

[a]Reference 11.
[b]All work is ours except matrix work from Ref. 5.
[c]Vertical detachment energy with respect to the neutral ground state.

TABLE IV. Comparison of geometries and energy separations of Ga_2As/Ga_2As^-.

Reference	Species	State	Level	θ (°)	Ga–As (Å)	Ga–Ga (Å)	ΔE (eV)	$\nu_1(a_1)$	$\nu_2(a_1)$	$\nu_3(b_2)$
Balasubramanian[a]	Ga_2As^-	$^1A_1$	MRSDCI	98.5	2.37		−2.20(−2.17)	240.5	46.5	275.3
	Ga_2As	$^2A'$	MRSDCI	90.3	2.83, 2.534		0.0(0.025)	182.7	50.4	265.6
	Ga_2As	$^2B_2$	MRSDCI	79.9	2.407		0.09(0.0)			
	Ga_2As	$^2B_1$	MRSDCI	108.2	2.52		0.16(0.22)	194.5	43.0	225.0
Theory	Ga_2As^-	$^1A_1$	B3LYP	106.3	2.384	3.816	−2.429	244	46.7	277
	Ga_2As	$^2B_2$	B3LYP	95.4	2.392	3.540	0.000	229	46.7	173.2*i*
Experiment[b]	Ga_2As^-	$^1A_1$	PES				−2.457±0.015	245		
	Ga_2As	*X*	PES				0.0			
	Ga_2As	*X*	MATRIX					160		204.7
	Ga_2As	*A*	PES				0.209±0.040	200		
	Ga_2As	*B*	PES				0.28	279		

[a]Reference 20.
[b]All work is ours except matrix work from Ref. 5.

observed. When a frequency and normal coordinate change satisfactorily reproduce the spectra, the origin of the transition is shifted by ±1 quanta of the neutral frequency and the frequency and normal coordinate change are reoptimized. Under these conditions, we have found that the experimental data is not as well-reproduced, so error bars for the band origin are assumed to be no larger than ±1 quanta of the active neutral frequency.

A. GaX_2

Our calculations and the earlier results listed in Tables I and II show both GaX_2^- species to have a $^1A_1$ ground state $(\dots 1b_1^2 4a_1^2 2b_2^2)$. One-electron detachment from the two highest lying orbitals results in the $\tilde{X}\,^2B_2$ ground and $\tilde{A}\,^2A_1$ excited neutral states, with all three anion and neutral states having C_{2v} symmetry. All ∠XGX bond angles are acute, implying strong X–X bonds. Term values for the $^2A_1$ state are calculated to be about 1 eV for GaP_2 and 0.7 eV for $GaAs_2$, in good agreement with the separation between the two bands in the experimental spectra (Fig. 3), and supporting the assignment of these bands in Sec. III.

The vibrational progressions of the $\tilde{X}\,^2B_2$ states of GaP_2 and $GaAs_2$ are very regular indicating that most of the FC activity is in one vibrational mode; its frequency is 220 cm^{-1} for GaP_2 and 177 cm^{-1} for $GaAs_2$. These values are close to the calculated frequencies for the ν_2 (Ga–X stretching) mode (Tables I and II). The dominance of this mode in the PE spectra is consistent with the calculated normal coordinate displacements. These are considerably larger than for the ν_2 mode than for the higher frequency ν_1 mode, since the largest geometry change upon photodetachment to this state is a lengthening of the Ga–X bond accompanied by a decrease in the XGaX bond angle. Our frequencies are also in excellent agreement with the infrared matrix experiments of Li *et al.*, where they report the $\omega_2(a_1)$ fundamentals to be 220.9 cm^{-1} and 174.1 cm^{-1} in GaP_2 and $GaAs_2$, respectively.[5] Hence the main vibrational progression in the $\tilde{X}\,^2B_2$ PE band of both species is assigned to the ν_2 mode.

Li *et al.* also observe infrared bands in the matrix absorption spectra of GaP_2 and $GaAs_2$ at 322 cm^{-1} and 231 cm^{-1}, respectively, and assigned both bands to the ν_1 fundamental. This assignment is at odds with the calculations in Tables I and II in which considerably higher ν_1 frequencies are predicted for both species: 690 cm^{-1} for GaP_2 and 382.5 cm^{-1} for $GaAs_2$.[20,31] On the other hand, the experimental IR frequencies are much closer to where the calculations would predict the $\nu_1\nu_2$ combination band to occur, 349 cm^{-1} for GaP_2 and 243 cm^{-1} for $GaAs_2$, ignoring anharmonic effects. Hence a reassignment of the matrix bands is appropriate.

The $\tilde{A}\,^2A_1$ bands of the GaX_2^- PE spectra are also dominated by a single progression with a frequency of 328 cm^{-1} for GaP_2 and 235 cm^{-1} for $GaAs_2$. Based on comparison with the calculated frequencies and normal coordinate displacements in Tables I and II, this progression is assigned to the ν_2 mode for both species. However, while the calculated magnitudes $|\Delta Q_{1,2}|$ are similar for detachment to the two states (see Table V), the signs of the two displacements are reversed because detachment to the $\tilde{A}\,^2A_1$ state results in a shorter Ga–X bond and larger XGaX bond angle.

Figure 7 shows the best fit simulations of the GaX_2^- photoelectron spectra. The parameters used in these fits are listed in Tables I and II. The $\tilde{X}\,^2B_2$ bands of GaP_2 and $GaAs_2$ are quite extended, making it difficult to pick out the origin by inspection, but based on our simulations the vibrational origins (indicated by arrows) and hence the electron affinities are 1.666±0.027 eV and 1.894±0.022 eV for GaP_2 and $GaAs_2$, respectively; the error bars correspond to 1 quantum of ν_2 vibration. Our value for GaP_2 is in good agreement with both calculated values in Table I obtained by DFT. For $GaAs_2$, the experimental electron affinity agrees better with our DFT value, 1.86 eV, than with the other values listed in Table II. Simulations of the $\tilde{A}\,^2A_1$ bands yields adiabatic detachment energies of 2.710±0.040 eV and 2.588±0.030 eV for GaP_2 and $GaAs_2$, respectively, yielding term values of 1.044±0.055 eV and 0.694±0.037 eV for the $\tilde{A}\,^2A_1$ state. The GaP_2 term value determined here agrees with our previously reported value[8,10] of 0.99 eV estimated by the difference in vertical detachment energies of the $\tilde{X}\,^2B_2$ and $\tilde{A}\,^2A_1$ states.

The PE spectrum showing the second excited $\tilde{B}\,^2B_1$ state of GaP_2 is not shown in the current paper, however we mention it briefly in order to reevaluate the term energy. We previously reported the adiabatic detachment energy of the *B*

TABLE V. Comparison of geometries and energy separations of $Ga_2As_3/Ga_2As_3^-$ and Ga_2P_3/Ga_2P_3.

Reference	Species	State	Level	P–P (Å)	Ga–Ga (Å)	Ga–P (Å)	ΔE (eV)	Frequencies (cm^{-1})[a]
Theory	$Ga_2P_3^-$	$^1A_1'$	B3LYP	2.248	4.488	2.593	−2.912	508,182 ($A1'$) 279 ($A2''$) 101,391 (E') 206 (E'')
	Ga_2P_3	$^2A_2''$	B3LYP	2.317	4.183	2.483	0.0	470, **210** ($A1'$) 243 ($A2''$) 117, 365 (E') 262 (E'')
Experiment	$Ga_2P_3^-$	$^1A_1'$	PES				−2.991	
	Ga_2P_3	$^2A_2''$	PES				0.0	213
				As–As (Å)	Ga–Ga (Å)	Ga–As (Å)		
Theory	$Ga_2As_3^-$	$^1A_1'$	B3LYP	2.486	4.619	2.719	−2.694 ±0.026	169,297 ($A1'$) 205 ($A2''$) 82,226 (E') 124 (E'')
	Ga_2As_3	$^2A_2''$	B3LYP	2.558	4.279	2.600	0.0	286, **190** ($A1'$) 184 ($A2''$) 100,220 (E') 164 (E'')
Experiment	$Ga_2As_3^-$	$^1A_1'$	PES				−2.783 ±0.024	
	Ga_2As_3	$^2A_2''$	PES				0.0	193

[a]Active vibrational mode in the PE spectrum is in boldface.

state origin to be 4.324±0.010 eV.[10] Subtracting the new electron affinity gives us the improved term value $T_0(^2B_1) = 2.603 \pm 0.029$ eV. In addition, recent calculations by Archibong *et al.*[31] confirm our assignments of the 500 and 589 cm^{-1} frequencies to the $\nu_1(a_1)$ mode of the neutral and anion, respectively, as well as our assignment of the 234 cm^{-1} frequency to the $\nu_2(a_1)$ mode of the neutral. All term values, vibrational frequencies, and assignments for GaP_2 and $GaAs_2$ are tabulated in Tables I and II, respectively.

Finally, we consider what the PE spectra reveal concerning the geometries of anion and neutral states of GaP_2 and $GaAs_2$. For GaP_2, the magnitudes of the ΔQ_i's used in our best-fit simulations are similar to those obtained from electronic structure calculations, with a slightly larger ΔQ_2 needed to fit the $^2B_2$ band, and a slightly smaller ΔQ_2 required for the $^2A_1$ band. Although our simulations do not depend on the sign of the ΔQ_i's, we assume the signs from the electronic structure calculations are correct. Hence, assuming the calculated anion geometries are correct, we can extract geometries for the $\tilde{X}\,^2B_2$ and $\tilde{A}\,^2A_1$ states from our signed values of the ΔQ_i's. These geometries are in fact quite close to the calculated geometries, and given the possible inaccuracies associated with our use of the parallel mode approximation we cannot claim that the structures obtained by our analysis represent an improvement over the calculations.

Our best-fit ΔQ_i values for detachment to the $\tilde{X}\,^2B_2$ state of $GaAs_2$ are in excellent agreement with those derived from Balasubramanian's[20] electronic structure values in Table II, indicating that his calculated geometries for the anion and neutral ground state are likely to be accurate. However, while the experimental frequency of 234 cm^{-1} for the $\tilde{A}\,^2A_1$ band agrees well with Balusubramanian's calculated frequency of 238.7 cm^{-1} for the ν_2 mode, the simulated ν_2 progression using his geometry is too long and ΔQ_2 must be reduced significantly, from 0.2302 to 0.130 Å amu$^{1/2}$. Converting our normal coordinate displacements to geometries (see Table VII) shows that the increase in bond angle and decrease in Ga–As bond length upon detachment to the $\tilde{A}\,^2A_1$ state are smaller than predicted in Balasubramanian's calculation.

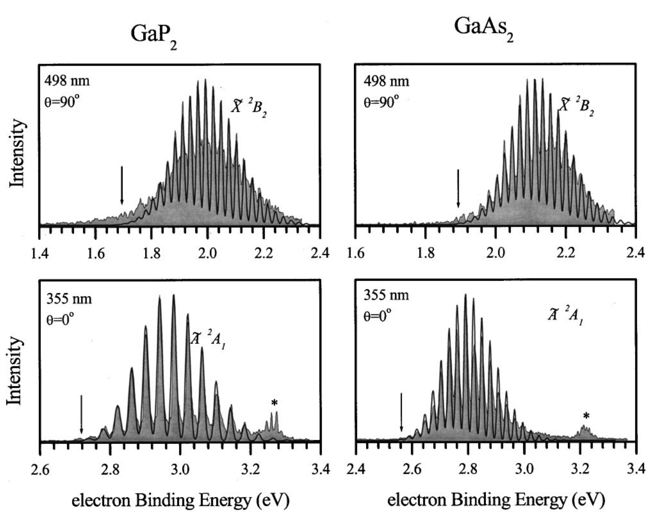

FIG. 7. Anion photoelectron spectra of GaX_2^- (gray solid) superimposed with FC simulation (black line).

B. Ga_2X

The experimental spectra in Fig. 4 and electronic structure calculations in Tables III and IV show that the Ga_2X^- PE spectra are more complex than the GaX_2^- spectra. The Ga_2X^- PE spectra show evidence for transitions to three neutral electronic states: the ground state, responsible for band *X*, and two low-lying excited states that result in the overlapped bands *A* and *B* in Fig. 4. While band *X* is of similar appearance in the Ga_2P^- and Ga_2As^- spectra, the excited state bands are quite different, with the somewhat surprising result that more vibrational structure is seen in the Ga_2As^- spectra. The overall appearance of the Ga_2P^- spectrum is very similar to the Al_2P^- PE spectrum.[36] This similarity suggests that the same state assignments for Al_2P be applied to Ga_2P, namely, that band *X* is the transition to the $\tilde{X}\,^2B_2$ ground state, while the vibrationally resolved band *A* and broad, unresolved band *B* result from transitions to the $\tilde{A}\,^2A_1$ and $\tilde{B}\,^2B_1$ excited state, respectively. Carrying this line of reasoning further, it is reasonable to assign band *X* in

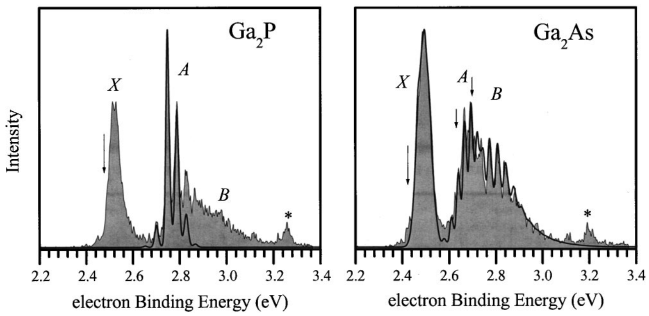

FIG. 8. Anion photoelectron spectra of Ga_2X^- (gray solid) superimposed with FC simulation (black line).

the Ga_2As^- spectrum to the transition to the $\tilde{X}\,^2B_2$ ground state of Ga_2As, with the excited state assignments being less obvious.

Confirmation of these assignments by comparison with electronic structure calculations is more problematic than for the GaX_2^- spectra. Our calculations on both Ga_2X^- anions yield a $^1A_1$ ground state with C_{2v} symmetry and the molecular orbital configuration $(\ldots 3a_1^2 1b_2^2 1b_1^2 2b_2^2)$. However, the neutral species are more complicated. Balasubramanian[20] find that Ga_2As has two nearly degenerate states: a $^2A'$ ground state of C_s symmetry, with unequal Ga–As bond lengths, and a $^2B_2$ state with C_{2v} symmetry. The $^2B_2$ state was found to be the ground state at the MRSDCI+Q level of theory, with the $^2A'$ state lying only 0.025 eV higher. Our DFT calculations on Ga_2P and Ga_2As yield a $^2B_2$ ground state when restricted to C_{2v} symmetry, but the ν_3 frequency is imaginary in both cases indicating that the C_{2v} structure is not an energy minimum. At the MRSDCI level, Feng[11] finds a $^2B_1$ ground state for Ga_2P and a $^2B_2$ excited state lying only 0.09 eV higher, but these calculations were restricted to C_{2v} symmetry.

We simulated the Ga_2As^- spectrum using Balasubramanian's geometries and frequencies for the anion and the $^2A'$ and $^2B_2$ neutral states[20] (since no frequencies are given for the neutral $^2B_2$ state, we used the anion vibrational frequencies), and the force constants from our DFT calculation on the anion. Simulation of the $^2A'$ state yields an extended progression in the ν_3 mode which would have been easily seen in our spectrum. On the other hand, simulation of the $^2B_2$ band using the *ab initio* parameters yields a single broad, unstructured peak, similar to the experimental band *X*. The width of the simulated peak depends strongly on the assumed anion temperature. The structured bands *A* and *B* were fit with anion temperature $T=250$ K (see below), so this temperature was also used to fit band *X*. The best-fit simulation, shown in Fig. 8, was obtained with the ΔQ_i values in Table VI, both of which are smaller than the corresponding *ab initio* values. Using Balasubramanian's anion geometry as a reference, the optimized geometry of the Ga_2As ground state is given in Table VII; it differs from Balasubramanian's calculated geometry for the neutral $^2B_2$ state (Table IV) in that its bond angle is about 13° larger. Nonetheless, assigning band *X* to the $^2B_2$ state is still reasonable since its calculated properties are in better agreement with experiment than any other state, and the same assignment holds for band *X* in the Ga_2P^- PE spectrum. Based on the simulation of band *X*, the electron affinity of Ga_2As is 2.428±0.020 eV, and we estimate the electron affinity of Ga_2P to be 2.481±0.020 eV.

The best-fit simulation of band *A* in the Ga_2P^- PE spectrum, shown in Fig. 8, yields anion and neutral frequencies of 385 and 328 cm^{-1}, respectively, for the ν_1 mode, with the

TABLE VI. Photoelectron spectra simulation parameters for active modes in Ga_2X^- and GaX_2^-.

Molecule	State	PES-FCF active modes ν_1 (cm^{-1})	ΔQ_1 (Å amu$^{1/2}$)[a]	ν_2 (cm^{-1})	ΔQ_2 (Å amu$^{1/2}$)[a]	Temp (K)
GaP_2^-	$^1A_1$	590		260		
GaP_2	$^2B_2$	690	0.029	222[b]	−0.220 (−0.188)	275
GaP_2	$^2A_1$	532	−0.023	328[b]	0.160 (0.186)	275
$GaAs_2^-$	$^1A_1$	330		198		
$GaAs_2$	$^2B_2$	386	0.033	176[b]	−0.191 (−0.189)	300
$GaAs_2$	$^2A_1$	312	−0.037 (−0.056)	235[b]	0.130 (0.230)	300
Ga_2P^-	$^1A_1$			375[b]		
Ga_2P	$^2B_2$		0.010		−0.181	
Ga_2P	$^2B_1$		0.051	311[b]	0.055	275
Ga_2As^-	$^1A_1$	46.5		240.5		250
Ga_2As	*X*		0.013 (0.043)		−0.191 (−0.4261)	250
Ga_2As	*A*	46.7	0.090 (0.183)	200[b]	0.061 (0.306)	250
Ga_2As	*B*		0.080	279[b]	0.065	

[a]Normal coordinate displacements from electronic structure calculations shown in parentheses when it is different from those used in the best-fit simulation.
[b]Observed experimental progression.

TABLE VII. Neutral structures based on best-fit normal coordinate displacements using calculated anion geometries as a reference.

Species	State[a]	θ (°)	Ga–P (Å)	P–P (Å)
GaP_2^-[b]	$^1A_1$	48.9	2.481	2.056
GaP_2	$^2B_2$	44.6	2.719	2.068
GaP_2	$^2A_1$	52.5	2.324	2.054
		θ (°)	Ga–As (Å)	As–As (Å)
$GaAs_2^-$[c]	$^1A_1$	52.7	2.586	2.296
$GaAs_2$	$^2B_2$	46.4	2.785	2.198
$GaAs_2$	$^2A_1$	56.9	2.489	2.373
		θ (°)	Ga–P (Å)	Ga–Ga (Å)
Ga_2P^-[d]	$^1A_1$	108.2	2.283	3.700
Ga_2P	(*X*) $^2B_2$	N/C		
Ga_2P	(*A*) $^2A_1$	109.1	2.327	3.798
		θ (°)	Ga–As (Å)	Ga–Ga (Å)
Ga_2As^-[e]	$^1A_1$	98.5	2.37	3.591
Ga_2As	(*X*) $^2B_2$	93.1	2.401	3.486
Ga_2As	(*A*) $^2B_1$	100.7	2.429	3.740

[a]For the Ga_2X species, the corresponding band in the PE spectrum is indicated in parentheses.
[b]Anion geometry from Ref. 31.
[c]Anion geometry from Ref. 11.
[d]Anion geometry from our DFT (B3LYP) calculation.
[e]Anion geometry from Ref. 20.

anion frequency derived from the hot band transition *a*. The frequency of the ν_2 mode was assumed to be 56 cm^{-1}, the same value as was calculated for the anion. The normal coordinate displacements ΔQ_1 and ΔQ_2 (Table VI) were chosen to reproduce the length of the progression and the widths of the individual peaks, respectively. The term value for the neutral state responsible for band *A* is 0.268 eV. As stated above, based on comparison with the Al_2P^- PE spectrum, this state is assigned as the $\tilde{A}\,^2A_1$ state. While this state has not been calculated for Ga_2P, we can determine its geometry from our normal coordinate displacements and the calculated anion geometry in Table III, assuming the signs of the ΔQ_i's are the same as for detachment to the $\tilde{A}\,^2A_1$ state of Al_2P;[49] this geometry is given in Table VII.

The differing anisotropy parameters for the overlapped bands *A* and *B* in the Ga_2As^- PE spectra confirm that they arise from transitions to distinct electronic states. The two bands were simulated by assuming activity in a single high frequency vibrational mode with a frequency of 200 cm^{-1} for band *A* and 279 cm^{-1} for band *B*, and an anion vibrational frequency of 245 cm^{-1}; these presumably correspond to the ν_1 modes for both states. In addition, a small ΔQ_2 value was used to match the experimental peak widths (Table VI). Term values for bands *A* and *B* were found to be 0.209 and 0.280 eV, respectively. The 200 cm^{-1} frequency for band *A* agrees with the calculated ν_1 frequency of 194.5 cm^{-1} for the $^2B_1$ state of Ga_2As.[20] Based on this comparison, one is tempted to assign band *A* to the $^2B_1$ state and band *B* to the $^2A_1$ state. However, the normal coordinate displacements used to simulate band *A* are noticeably smaller than those found using Balasubramanian's anion and neutral geometries. As a consequence the change in bond angle upon photodetachment (Table VII) is considerably smaller than predicted by his calculations, so this assignment, like the assignment of band *X*, is reasonable but not as compelling as the assignments made for the GaX_2^- spectra.

C. Ga_2X_2

The anion photoelectron spectra of $Ga_2X_2^-$ at 355 nm are not vibrationally resolved, even using the liquid-nitrogen cooled ion source configuration. We can nonetheless discuss band assignments based on calculations by Archibong and St-Amant[32] on $Ga_2P_2^-$ and our PE spectra of isovalent $Al_2P_2^-$.[36] The absence of vibrational structure in the $Ga_2X_2^-$ PE spectra is at first surprising, given that clear vibrational structure was seen in the PE spectra of Si_4^- and Ge_4^-.[12,13,50] However, while photodetachment of Si_4^- and Ge_4^- involves transitions between planar rhombus (D_{2h}) geometries of the anion and neutral species, the calculations by Archibong on Ga_2P_2 and Al_2P_2 indicate that the anion ground states of both species are nonplanar, distorted tetrahedral $^2B_1$ states with C_{2v} symmetry, the ^1A_g neutral ground states have planar rhombus geometries, and most of the low-lying excited neutral states have C_{2v} structures.[32,51] Hence, large changes upon the dihedral angle upon photodetachment can result in extensive progressions in the low-frequency umbrella (ν_3) mode that would not be resolved in our spectrum, since its calculated frequency is around 50 cm^{-1} in the various Ga_2P_2 anion and neutral states. On the basis of calculated energetics, band *X* in the $Ga_2P_2^-$ spectrum was assigned[32] to a transition from the anion $^2B_1$ state to the neutral ^1A_g ground state, while the more intense band *A* was assigned to a transition to the neutral $^3B_2$ state with a distorted tetrahedral structure.

The $Ga_2P_2^-$ and $Al_2P_2^-$ are similar in that each has a low intensity peak (band *X*) at low eBE followed by a more intense band (band *A*) at higher eBE. However, band *A* in the $Al_2P_2^-$ spectrum is vibrationally resolved with a distinct progression in the 320 cm^{-1} ν_2 mode and was assigned to the neutral $^3A_2$ state.[36] The calculated dihedral angle for this state was only 10° larger than in the anion, and simulations showed that progressions in the low-frequency umbrella mode were not long enough to wash out the higher frequency ν_2 progression. The absence of an analogous progression in band *A* of the $Ga_2P_2^-$ spectrum suggests a larger change in dihedral angle upon photodetachment to the neutral excited state. Unfortunately these angles were not given in Archibong's paper on Ga_2P_2 species.

D. Ga_2X_3

The $Ga_2X_3^-$ PE spectra are each dominated by a single band (*X*) which shows a well-resolved progression in a single vibrational mode for both species. This band presumably results from a photodetachment transition between anion and neutral states of the same symmetry, with geometry changes that activate only one totally symmetric mode in the PE spectrum. Electronic structure calculations on Ga_2As_3 predict a $^2A_2''$ ground state in D_{3h} symmetry with a trigonal bipyramidal structure,[19,26,34] while calculations on Ga_2P_3 predict a similar state to be nearly degenerate with a Jahn–Teller distorted $^2B_1$ state.[21] In addition, matrix electron spin resonance experiments on Ga_2As_3 indicate a D_{3h} structure.[6] The appearance of band *X* in the PE spectra is therefore consistent with the anions of both species having trigonal bipyramidal structures, and our DFT electronic structure calculations (Table V) find this to be the case, with $^1A_1'$ closed shell ground states found for both anions. Our DFT calculations for the neutral species yield states with geometries very similar to the $^2A_2''$ states calculated previously.

Simulations of band *X* for both species are shown in Fig. 9. The geometries and frequencies used in these simulations are very close to those obtained in our DFT calculations. Hence the simulations confirm that band *X* results from transitions between trigonal bipyramidal structures of the anion and neutral. The vibrational origins of band *X* occur at 2.991 ± 0.026 eV for $X = P$ and 2.783 ± 0.024 eV for $X = As$, in reasonable agreement with our calculated energetics.

The simulations are dominated by a progression in the ν_2 mode, a totally symmetric Ga–Ga stretch mode activated by the substantial decrease in the Ga–Ga bond length upon photodetachment. This is consistent with the nature of the a_2'' orbital from which detachment occurs, which is antibonding between the apical Ga and equatorial P atoms.[34] We note that the photoelectron spectrum of Si_5^- also shows vibrational structure attributed to similar structures and geometry changes upon photodetachment.[13]

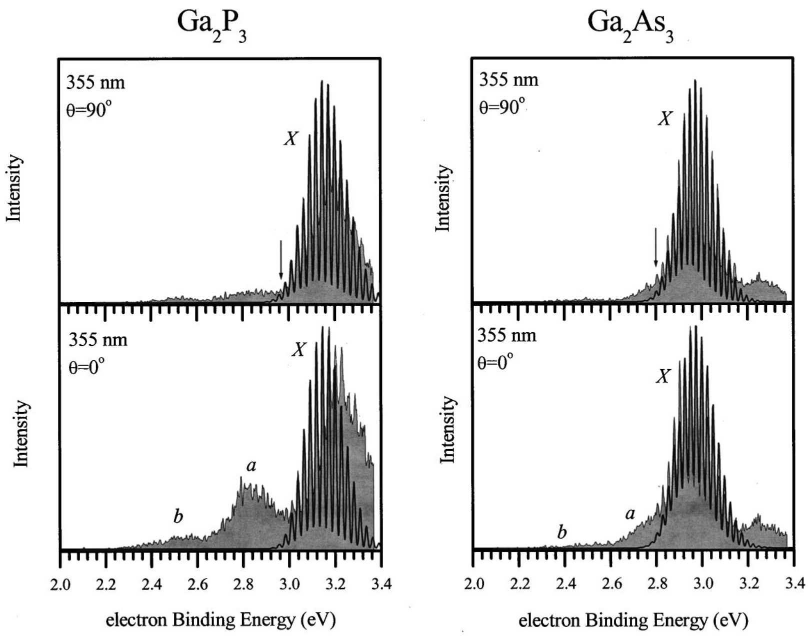

FIG. 9. Anion photoelectron spectra of $Ga_2X_3^-$ (gray solid) superimposed with FC simulation (black line).

The vibrational origins given above correspond to the electron affinities of Ga_2P_3 and Ga_2As_3 only if band *X* represents the transition between the anion and neutral ground electronic states. The presence of bands *a* and *b* complicates this issue. The photoelectron angular distributions associated with these bands differs from that of band *X*, with the relative intensities of bands *a* and *b* clearly higher at $\theta=0°$ than at $\theta=90°$. Hence, these two bands must arise from a different electronic photodetachment transition than band *X*, although it is less clear if they themselves arise from two distinct electronic transitions or instead represent a single extended transition.

There are several possible origins for these bands. They can originate from low-lying excited electronic states of the anion, or from transitions to lower-lying neutral states than the $^2A_2''$ D_{3h} state responsible for band *X*. As mentioned above, calculations by Feng[21] on Ga_2P_3 predict a $^2B_1$ state to be nearly degenerate with the $^2A_2''$ state; the $^2B_1$ state arises from Jahn–Teller distortion of a low-lying $^2E'$ state of Ga_2P_3. It is certainly possible that bands *a* and *b*, which show no vibrational structure, arise from photodetachment from the anion ground state to this $^2B_1$ state, since a transition to a structure of different symmetry generally results in the activation of multiple vibrational modes. However, the apparent origin of band *b* is more than 0.5 eV below that of band *X* in the $Ga_2P_3^-$ PE spectrum, about an order of magnitude larger than the calculated splitting between the $^2B_1$ and $^2A_2''$ states. Alternatively, since Feng's calculation on neutral Ga_2P_3 indicates the presence of a low-lying, unfilled e' orbital, there is likely to be a low-lying $^3E'$ electronic state of the anion which can undergo Jahn–Teller distortion, and transitions from this state to the neutral $^2A_2''$ state are also possible candidates for bands *a* and *b*. Similar considerations apply to the $Ga_2As_3^-$ PE spectra, although no low-lying $^2E'$ states were found in calculations on Ga_2As_3.[19] Finally, bands *a* and *b* bear some resemblance to the PE spectra of the tetra-atomic $Ga_2X_2^-$ species, even if they occur at somewhat lower eBE than the bands in the $Ga_2X_2^-$ PE spectra. Hence these bands may result from photodissociation to vibrationally hot $Ga_2X_2^-$ fragments followed by photodetachment of these fragments. This explanation is consistent with the observation that bands *a* and *b* are not seen at 266 nm.

V. CONCLUSIONS

We have presented and discussed the anion photoelectron spectra of GaX_2^-, Ga_2X^-, $Ga_2X_2^-$, and $Ga_2X_3^-$ (X=P,As). With the aid of electronic structure calculations and Franck–Condon simulations, we identify the structural and electronic symmetry of the electronic states observed and where possible have assigned the vibrational modes. The GaX_2^- anion and neutral species are shown unambiguously to be of C_{2v} symmetry and we assign the two neutral states observed to the $\tilde{X}\,^2B_2$ and $\tilde{A}\,^2A_1$ states.

Assignments of the ground and excited state bands in the Ga_2P^- and Ga_2As^- PE spectra were based on comparison to recent experimental work on Al_2P^- as well as electronic structure calculations, with all assigned anion and neutral states having C_{2v} symmetry. The Ga_2X species appear to be problematic from the perspective of electronic structure calculations, so the assignments are not as firm as for the GaX_2 species. The absence of vibrational structure in the $Ga_2X_2^-$ PE spectra is discussed in light of recent calculations predicting a nonplanar, distorted tetrahedral ground state for the $Ga_2P_2^-$ anion, in contrast to the planar rhombus structures found for Si_4^- and Ge_4^-. Finally, the dominant bands in the $Ga_2X_3^-$ spectra are vibrationally resolved and are attributed to transitions between anion and neutral states with trigonal bipyramidal geometries, similar to Si_5^-.

ACKNOWLEDGMENT

This research is supported by the National Science Foundation under Grant No. DMR-9814677.

[1] P. P. Jenkins, A. N. Macinnes, M. Tabibazar, and A. R. Barron, Science **263**, 1751 (1994).
[2] S. C. O'Brien, Y. Liu, Q. Zhang, J. R. Heath, F. K. Tittel, R. F. Curl, and R. E. Smalley, J. Chem. Phys. **84**, 4074 (1986).
[3] Y. Liu, Q. L. Zhang, F. K. Tittel, R. F. Curl, and R. E. Smalley, J. Chem. Phys. **85**, 7434 (1986).
[4] C. Jin, K. J. Taylor, J. Conceicao, and R. E. Smalley, Chem. Phys. Lett. **175**, 17 (1990).
[5] S. Li, R. J. Van Zee, and W. Weltner, J. Phys. Chem. **97**, 11393 (1993).
[6] R. J. Van Zee, S. Li, and W. Weltner, Jr., J. Chem. Phys. **98**, 4335 (1993).
[7] S. Schlect, R. Schaefer, J. Woenckhaus, and J. A. Becker, Chem. Phys. Lett. **246**, 315 (1995).
[8] T. R. Taylor, K. R. Asmis, C. Xu, and D. M. Neumark, Chem. Phys. Lett. **297**, 133 (1998).
[9] K. R. Asmis, T. R. Taylor, and D. M. Neumark, Chem. Phys. Lett. **308**, 347 (1999).
[10] T. R. Taylor, K. R. Asmis, H. Gomez, and D. M. Neumark, Eur. Phys. J. D **9**, 317 (1999).
[11] P. Y. Feng and K. Balasubramanian, Chem. Phys. Lett. **265**, 41 (1997).
[12] T. N. Kitsopoulos, C. J. Chick, A. Weaver, and D. M. Neumark, J. Chem. Phys. **93**, 6108 (1990).
[13] C. Xu, T. R. Taylor, G. R. Burton, and D. M. Neumark, J. Chem. Phys. **108**, 1395 (1998).
[14] K. Balasubramanian, J. Chem. Phys. **87**, 3518 (1987).
[15] K. Balasubramanian, Chem. Rev. **90**, 93 (1990).
[16] K. Balasubramanian, Chem. Phys. Lett. **171**, 58 (1990).
[17] K. K. Das and K. Balasubramanian, J. Chem. Phys. **94**, 6620 (1991).
[18] D. W. Liao and K. Balasubramanian, J. Chem. Phys. **96**, 8938 (1992).
[19] M. Z. Liao, D. G. Dai, and K. Balasubramanian, Chem. Phys. Lett. **239**, 124 (1995).
[20] K. Balasubramanian, J. Phys. Chem. **104**, 1969 (2000).
[21] P. Y. Feng and K. Balasubramanian, Chem. Phys. Lett. **265**, 547 (1997).
[22] P. Y. Feng and K. Balasubramanian, Chem. Phys. Lett. **258**, 387 (1996).
[23] P. Y. Feng and K. Balasubramanian, Chem. Phys. Lett. **288**, 1 (1998).
[24] R. M. Graves and G. E. Scuseria, J. Chem. Phys. **95**, 6602 (1991).
[25] M. A. Al-Laham and K. Raghavachari, Chem. Phys. Lett. **187**, 13 (1991).
[26] L. Lou, L. Wang, L. P. F. Chibante, R. T. Laaksonen, P. Nordlander, and R. E. Smalley, J. Chem. Phys. **94**, 8015 (1991).
[27] L. Lou, P. Nordlander, and R. E. Smalley, J. Chem. Phys. **97**, 1858 (1992).
[28] W. Andreoni, Phys. Rev. B **45**, 4203 (1992).
[29] V. Tozzini, F. Buda, and A. Fasolino, Phys. Rev. Lett. **85**, 4554 (2000).
[30] U. Meier, S. D. Peyerimhoff, and F. Grein, Chem. Phys. **150**, 331 (1991).
[31] E. F. Archibong and A. St-Amant, Chem. Phys. Lett. **316**, 151 (2000).
[32] E. F. Archibong and A. St-Amant, Chem. Phys. Lett. **330**, 199 (2000).
[33] R. Arratia-Perez and L. Hernandez-Acevedo, J. Chem. Phys. **110**, 10882 (1999).
[34] R. Arratia-Perez and L. Hernandez-Acevedo, J. Chem. Phys. **109**, 3497 (1998).
[35] I. Vasiliev, S. Ogut, and J. R. Chelikowsky, Phys. Rev. B **60**, R8477 (1999).
[36] H. Gomez, T. R. Taylor, and D. M. Neumark, J. Phy. Chem. A **105**, 6886 (2001).
[37] R. B. Metz, A. Weaver, S. E. Bradforth, T. N. Kitsopoulos, and D. M. Neumark, J. Phys. Chem. **94**, 1377 (1990).
[38] C. Xu, G. R. Burton, T. R. Taylor, and D. M. Neumark, J. Chem. Phys. **107**, 3428 (1997).
[39] B. A. Mamyrin and D. V. Shmikk, JETP **49**, 762 (1979).
[40] G. Markovich, R. Giniger, M. Levin, and O. Cheshnovsky, J. Chem. Phys. **95**, 9416 (1991).
[41] J. Cooper and R. N. Zare, in *Lectures in Theoretical Physics*, edited by S. Geltman, K. T. Mahanthappa, and W. E. Brittin (Gordon and Breach, New York, 1969), Vol. XI-C, p. 317.
[42] K. M. Ervin and W. C. Lineberger, in *Advances in Gas Phase Ion Chemistry* (JAI, New York, 1992), Vol. 1, p. 121.
[43] H. Gomez, T. R. Taylor, K. R. Asmis, and D. M. Neumark (in preparation).
[44] M. J. Frisch, G. W. Trucks, H. B. Schlegel *et al.*, GAUSSIAN 98 (Gaussian, Inc., Pittsburgh, 1998).
[45] T. H. Dunning, Jr., J. Chem. Phys. **90**, 1007 (1989).
[46] R. A. Kendall, T. H. Dunning, and R. J. Harrison, J. Chem. Phys. **96**, 6796 (1992).
[47] C. Lee, W. Yang, and R. G. Parr, Phys. Rev. B **37**, 785 (1988).
[48] A. D. Becke, J. Chem. Phys. **98**, 1372 (1993).
[49] P. Y. Feng and K. Balasubramanian, Chem. Phys. Lett. **318**, 417 (2000).
[50] G. R. Burton, C. Xu, C. C. Arnold, and D. M. Neumark, J. Chem. Phys. **104**, 2757 (1996).
[51] E. F. Archibong, R. M. Gregorius, and S. A. Alexander, Chem. Phys. Lett. **321**, 253 (2000).